Control Software Optimization for a Multi-Clutch System in a Hybrid All Wheel Drive Vehicle

Roberta Cavalcanti [*], **Germano Sandoni** [**,1], **Roberto Zanasi** [***]

[*] *AVL List GmbH, Hans-List-Platz 1, 8020 Graz, Austria*
E-mails: roberta.cavalcanti@avl.com

[**] *MAGNA STEYR Fahrzeugtechnik, MSF/EHFF Liebenauer Hauptstrasse 317, 8041 Graz, Austria*
Phone: +43 664 8840 5612, Fax: +43 316 404 5955
E-mails: germano.sandoni@magnasteyr.com

[***] *DII, University of Modena and Reggio Emilia, Via Vignolese 905/b, 41100 Modena, Italy.*
E-mail: roberto.zanasi@unimore.it

Abstract: The hybrid vehicles are already since some years on the market, with the target of reducing fuel consumption and emission. An innovative four wheel drive hybrid drivetrain was developed in MAGNA STEYR, with the additional aim to improve performances and safety. The prototype vehicle which is mentioned in this paper consists of two electric motors and four hydraulically controlled clutches, in order to obtain different drivetrain configurations (Parallel, Serial-hybrid, etc.). The electronic control of these clutches is a particular critical point to ensure the functionality of the system. In the paper, the main principles concerning the hardware structure, the particular software architecture and the results which became important during the development of a first car prototype are mentioned and described.

1. INTRODUCTION

Nowadays modern cars research is oriented in developing alternative powertrain systems, aimed at saving resources, reducing emission, increasing performance and functionality. A key role in the modern development of a vehicle is played by the design of mechanics combined with electronic hardware and software. Hybrid powertrain systems combine standard combustion engines with electrical motors, in order to improve driving dynamics and allowed electric torque vectoring. The main advantage of an hybrid structure is that, with the help of the electric motors, the Internal Combustion Engine (ICE) is torque compensated and it is brought to work in the optimal point, that minimizes the comsuption/emission (see AVLConference (2007)). Other advantages are the high comfort obtained through the electrical launch and the high efficiency in traffic with the start/stop of the ICE. Moreover there is the possibility of recuperating energy during braking. With an hybrid driveline also the car performances can be increased: an electrical boost can improve accelcration, handling and the gear shifting can be done without torque lack, simply delivering torque on the electric front axle, etc. All these advantages normally are able to compensate the higher costs of the hybrid vehicles, the increased weight and the more space required by the hybrid transmission (see Babiel (2007)). In this new field, it is very important to develop an efficient electronic control of the hybrid driveline. In this paper the main characteristics of an innovative hybrid driveline are discussed and presented, with particular attention at the electro-hydraulic actuation system and the software realization (see dSpaceNews (2008)). All the main components of this actuator system have been modelled by using a graphical technique, named Power-Oriented Graphs (POG). By keeping "coupled" the variables which are "conjugate" with respect to power flow, this graphical technique provides block dynamic models which, usually, are intuitive and easy to use. For a more detailed description of the POG graphical technique, please refer to Zanasi (1991) and Zanasi (1994). A control strategy that combines a standard PID controller and a lead compensator is developed, on the basis of the linearized model of the hydraulic system. The effectiveness of the control strategy has been tested in simulation, using the presented POG nonlinear model, and results have been compared with the real data obtained on a demo vehicle.

The paper is organized as follows: the Hybrid Powertrain is presented in Section 2 and the general proposed software architecture is shown in Section 3. The hydraulic actuator system and the control requirements are described in Section 4, together with the POG dynamic model. A simple PID pressure controller, the linear analysis and the synthesis of a lead lag compensator are described in Section 5. Simulation and experimental results, that validate the proposed control strategies, are shown in Section 6.

[1] Corresponding Author.

2. HYBRID POWERTRAIN DESCRIPTION

The structure of the considered Hybrid Powertrain is shown Fig. 1: note that an Electric Four Wheel Drive module (E4WD module) has been added at the traditional longitudinal driveline topology, between the Internal Combustion Engine (ICE) and the Automate Manual Transmission gearbox (AMT).

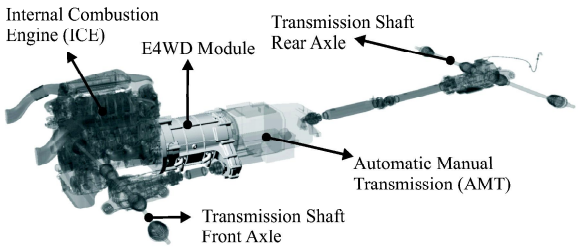

Fig. 1. Structure of the Hybrid Driveline.

A positive aspect of this solution is the high level of integration, which allows flexibility and modularity in the construction. The basic functional principles of the hybrid powertrain and the mentioned E4WD module are shown in Fig. 2. The structure of the electro-mechanical system consists of two electric motors EM_1, EM_2 and four wet multi-disk clutches hydraulically actuated C_1, ..., C_4. For security reasons the clutches C_1, C_2 are normally closed, with a preloaded spring, while the clutches C_3 and C_4 are normally opened.

The torque flows from the ICE towards the wheels through: the Torsional Vibrator Dumper (TVD), the clutch C_2, the electric motor EM_1, the clutch C_1, the electric motor EM_2, the AMT gearbox and the Rear Differential (RD). This corresponds to the typical parallel hybrid configuration. Through the two $DC/AC_{1,2}$ converters it is possible to get/store energy from/towards the battery (ES=Energy Storing system). The typical serial hybrid configuration is obtained by keeping opened the clutches C_1 and C_4, closed the clutches C_2 and C_3. The electrical motor EM_2 brings torque at the front differential (FD), passing through the Chain Drive (CD), while the ICE and the EM_1, used as generator, load the battery system.

The proposed hybrid powertrain configuration is very flexible and, due to the presence of the clutch C_4, both the electrical motors can be used to drive torque towards the front or rear axles.

3. SOFTWARE ARCHITECTURE CONCEPT

The control software architecture proposed to bring and keep, in every driving situation, the Hybrid Transmission at the optimal working point is shown in Fig. 3.

The driver wishes, coming from the gas pedal, the brake pedal, the gear level and the steering wheel position, are combined with the dynamic state of the vehicle (velocity, yaw rate, slip angle, etc.) and evaluated in the Vehicle Controller module (ESP).

This ESP module is designed to optimize the traction and to translate the driver wishes in torques on the front/ rear

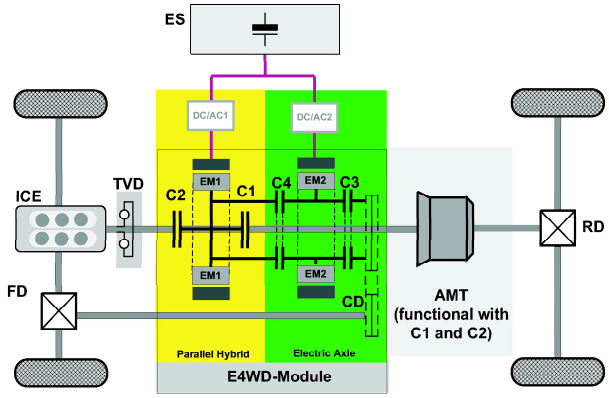

Fig. 2. Hybrid Powertrain Schematization.

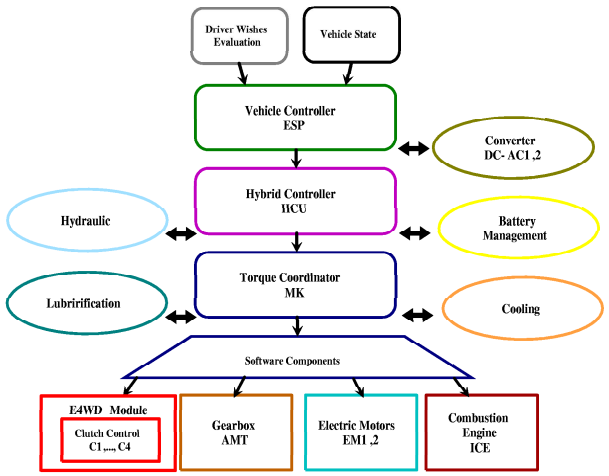

Fig. 3. Proposed Control Modular Software Architecture for Hybrid Transmission and Energy Management.

axles, taking in consideration the availability of the request torques.

The requested axles torques are passed to the Hybrid Control Unit module (HCU) which, on the basis of global efficiency, thermal condition, charge of the battery, comfort and dynamic state, decides how to divide the torques between the different components (EM_1, EM_2, ICE) and calculates the actual gear and the torques transmitted through the clutches $C_1, ..., C_4$.

The main goal of the Torque Coordinator module (MK) is to handle and control the transient situations (e.g. launch, gear shift) and to apply the pseudo stationary HCU requested torques/gear directly at the different components.

The different Software Components are shown in Fig. 3. They have been designed to control the Gearbox, the E4WD module, the Electric Motors EM_1, EM_2 and the Internal Combustion Engine (ICE), in such a way that the reference signals of the torque coordinator are followed as fast as possible.

In particular the E4WD module is composed of the six software modules shown in Fig. 4. It is important to observe that the Clutch Control modules $C_1, ..., C_4$ have basically the same structure: they are just replayed and recalibrated with different parameters, to cope with the physical characteristics of the different clutches.

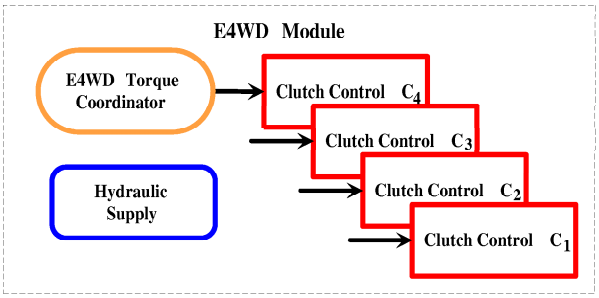

Fig. 4. E4WD Module Software Architecture.

This modularity and reusability of the Clutch Control Software is possible and it is particularly important, that the controller is well implemented, in order to obtain good accuracy and performance in the clutches transmitted torques. This clutch controller optimization will be discussed in Section 5.

4. ELECTRO-HYDRAULIC SYSTEM DESCRIPTION AND POG MODEL OF THE E4WD MODULE

As shown in Fig. 5, the four multi-disk wet clutches are hydraulically actuated and electronically controlled. The pressure supply system (HPU) consists of an hydraulic pump, an accumulator and a tank mounted on the vehicle front and connected to the valves block by means of hydraulics lines.

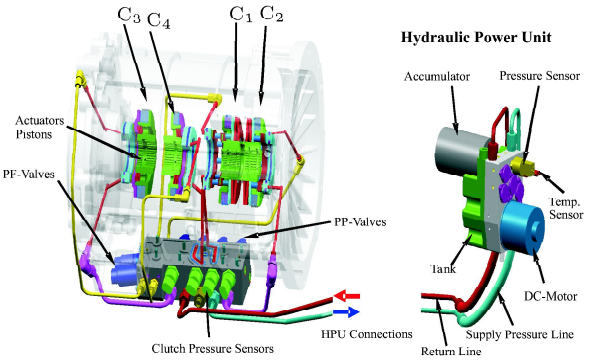

Fig. 5. E4WD Module Actuation System and Hydraulic Power Unit (HPU).

An hydraulic schematization of the E4WD module is shown in Fig. 6. This module is composed of the following parts: storage tank, DC Motor and pump, Power Unit that includes a pressure accumulator, four proportional pressure valves (PP-Valve) that control the clutches actuator pistons and hydraulic connection tubes. For security reasons, two proportional flow valves (PF-Valve) have been inserted in the system, in order to reduce the actuators pressures, when danger situations occur. Pressure sensors P_1, ..., P_4 are used to accurately control the clutches transmitted torques.

The POG dynamic model of the Hydraulic Actuation System is shown in Fig. 6. To be observed the one to one correspondence between the POG model blocks and

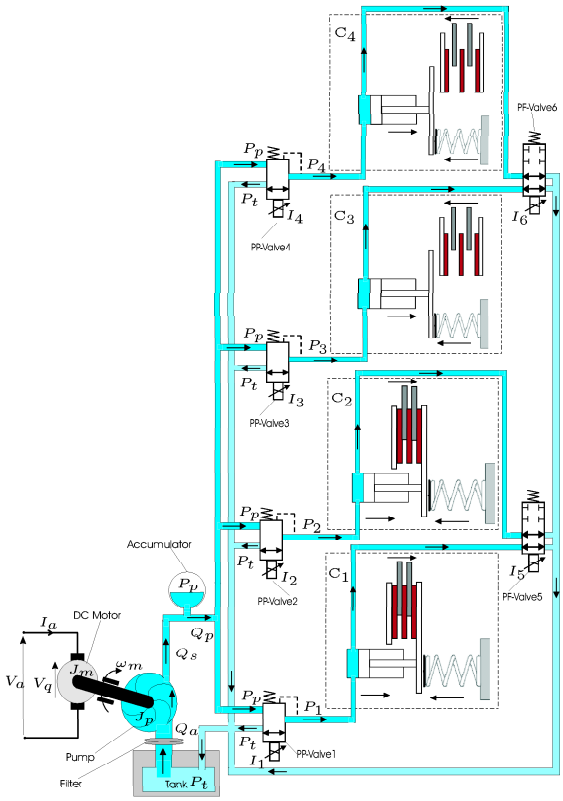

Fig. 6. Schematization of the Hydraulic Actuation System of the E4WD Module.

the physical components of the hydraulic actuator. The main variables and parameters that appear in the model are: V_a is the DC motor supply voltage, I_a is the motor armature current, k_m is the DC motor gain, V_q is the rotor field voltage, ω_m is the DC motor angular velocity, T_m is the motor torque, T_p is the resistant torque of the pump, b_m and b_p are the viscous friction coefficients of the DC motor and the pump, J_m and J_p are the inertia moment of the DC motor and the pump, b_{cm} is the coulomb friction of the pump, k_P is the constant gain of the pump, Q_a is the flow rate supplied by the pump, Q_l is the leakage flow rate of the pump, Q_s is the oil flow rate that recharges the accumulator, $Q_p = Q_{p1} + Q_{p2} + Q_{p3} + Q_{p4}$ is the total flow rate absorbed by the four clutches C_1, ..., C_4, V_0 is the total volume of the accumulator, V_f is the oil volume inside the accumulator, P_p the power supply pressure, P_t is the return pressure, P_1 is the actuator pressure, x_{s_1} is the valve spool position (function of the valve current I_1), x_c is the actuator position, F_c is the hydraulic force on the piston, C_d is the hydraulic capacity of the actuator chamber, k_V is the hydraulic valve constant, $k_c(x_c)$ is a nonlinear function describing the stiffness of the spring and the clutch disks as a function of position x_c, m_c is the piston mass, b and b_c are the linear friction and coulomb friction coefficients of the piston actuator, A_c and A_v are the actuator and valve areas, Q_v is the fluid flow rate at the valve output. In Fig. 7 only the clutch C_1 has been modelled. The POG model of the other four clutches C_2, C_3 and C_4 can be obtained in a similar way. For a detailed description of the POG model, and a more accurate analysis of the hydraulic system, please refer to Zanasi (2003) and Cavalcanti (2007).

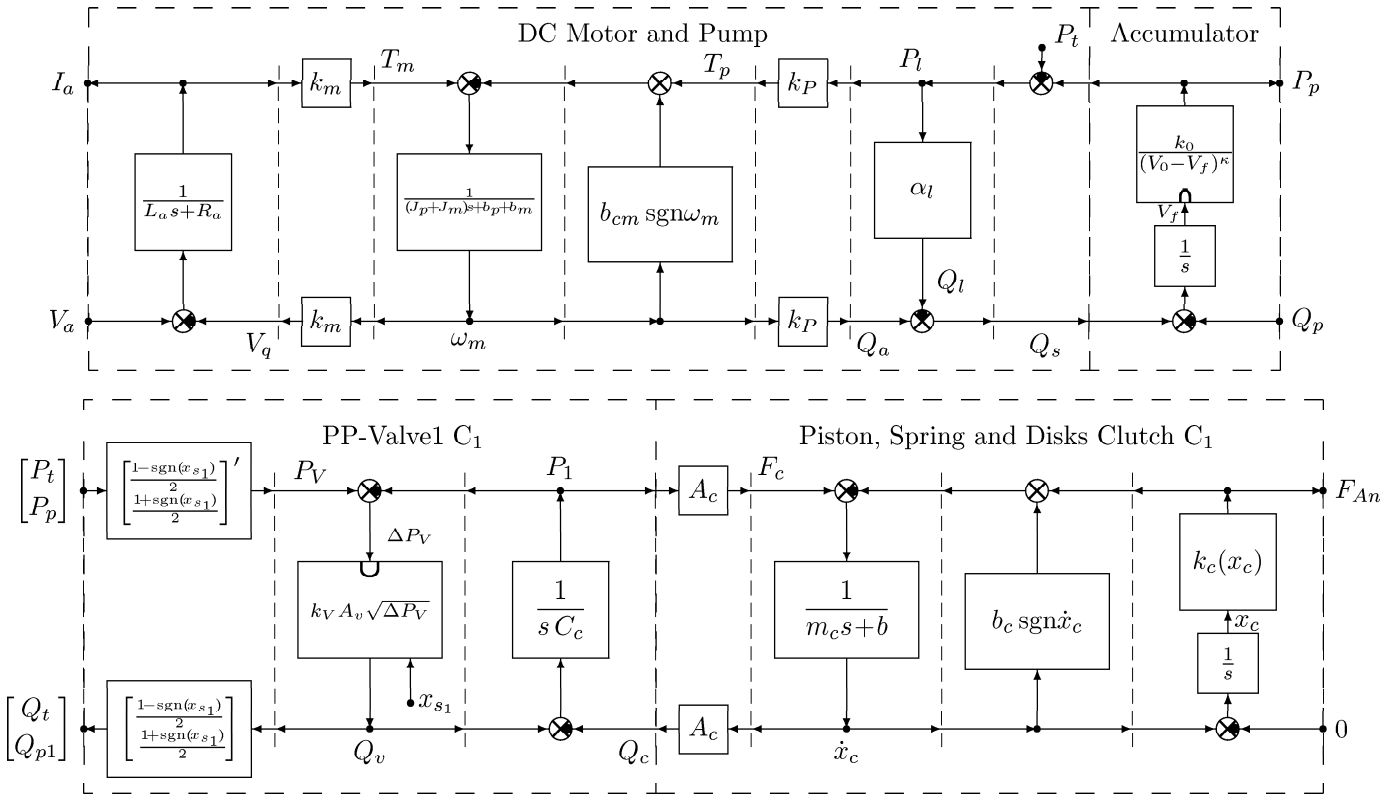

Fig. 7. POG model of the E4WD Module Hydraulic Actuator System.

4.1 Model Parameter Identification

In order to precisely identify the parameters of the POG model, different tests have been executed. In particular Fig. 8 shows the open loop step response of the actuator pressure P_1, for different values of the valve current: $I_1 = 0.7$A, $I_1 = 1.1$A and $I_1 = 1.25$A. Fig. 8 clearly shows that the simulation results obtained with the POG model are very similar to real values measured on the system.

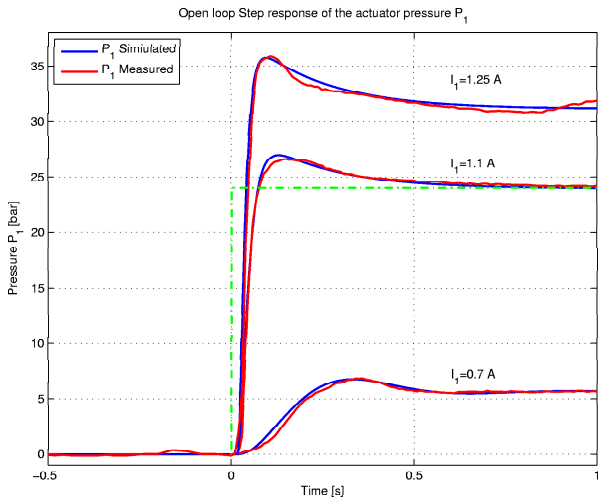

Fig. 8. Step responses of the actuator pressure P_1: simulated (blue) vs. measured (red).

5. PRESSURE CONTROL LOOP

The control software architecture used for controlling the clutch actuator is shown in Fig. 9. It is a cascade control structure preceded by an open loop torque controller. This first control module is used for performing different tasks: it pre-filters the requested torque T_{r1} coming from the Torque Coordinator, it transforms this signal in a pressure reference signal P_{r1} for the pressure controller, it compensates the hysteresis of the clutch characteristic (actuator pressure-transmitted torque) and it determines the clutch "kiss point". In the outer control loop a standard PID controller is used (see magenta block) to keep the actuator pressure P_1 as close as possible to the reference signal P_{r1}. The inner control loop is used for controlling the valve current I_1 towards the reference signal I_{r1}, in order to improve the time response of the pressure proportional valve (PP-Valve). The general structure of the PID pres-

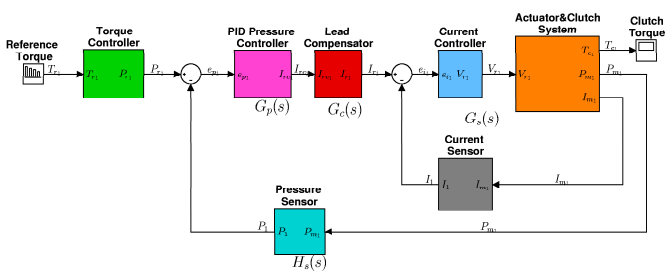

Fig. 9. Clutch Actuator Control Software Structure.

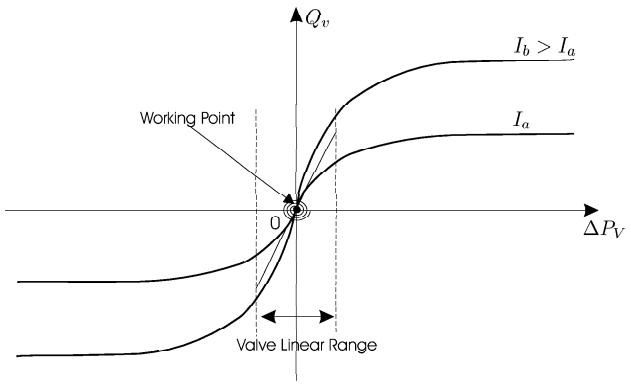

Fig. 10. Valve linearization in the working point.

sure controller, used in the outer loop, is composed of proportional, integral and derivative parts:

$$G_p(s) = \frac{I_{rc}(s)}{E_p(s)} = K_p + \frac{K_i}{s} + K_d\, s$$

The parameters of this PID Pressure Controller have been calibrated empirically. Moreover, for improving the performance/ stability of the controlled system, an additional Lead Compensator $G_c(s)$ (see red block) has been introduced in the outer loop:

$$G_c(s) = \frac{I_{r_1}(s)}{I_{rc_1}(s)} = K_c\, \frac{1+\tau_1 s}{1+\tau_2 s}$$

with $\tau_1 > \tau_2$. The stabilization effect of this compensator is due to the phase lead ϕ introduced at frequency $\overline{\omega} = \frac{1}{\sqrt{\tau_1 \tau_2}}$. For having a good phase margin for the close loop system a correct calibration of the $G_c(s)$ is necessary (see Section 5.2), but for doing this calibration the linear analysis described in the next Section 5.1 is needed.

5.1 POG Model Linearization

The modelled hydraulic system is highly nonlinear. The main nonlinearity are: the quadratic characteristics of the hydraulic valve (see Fig. 10), the static/coulumb friction of the valves spools and actuators pistons, the magnetic saturation of the valves coils, etc. Despite of all these nonlinear effects, when the system works in a very small area close to a fixed point, in the neighborhoods of this point the system can be linearized. In the case of movements also the static frictions can be, in a first approximation, neglected. The current control loop can be linearized and included in the actuator model. The whole actuator system will be represented using the transfer function $G_s(s)$. The pressure sensor has a very fast dynamics, which can be described using the transfer function $H_s(s)$. Due to the linearization, the parameters of the two transfer functions $G_s(s)$ and $H_s(s)$ are dependent of the working point. The Bode diagrams of the open loop system $G_T(s) = G_p(s)G_s(s)H_s(s)$, when the valve current is $I_1 = 1.1$A, is shown in Fig. 11 (see blue line). It is possible to observe that using the simple PID pressure controller $G_p(s)$, the system is stable with phase and gain margins of $M_\phi = 135°$ and $M_\alpha = 50$ dB. The Bode diagrams of the closed loop system $G_0(s) = \frac{G_T(s)}{1+G_T(s)}$ is shown in Fig. 12 (see blue line). The bandwidth of the closed loop system $G_0(s)$ is only 4 rad/s and it can be significantly improved with the introduction of a lead compensator $G_c(s)$.

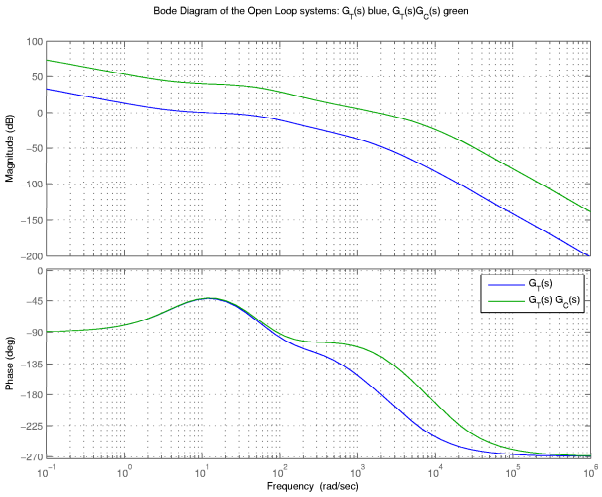

Fig. 11. Bode diagrams of the open loop system $G_T(s)$, with and without the lead compensator $G_c(s)$.

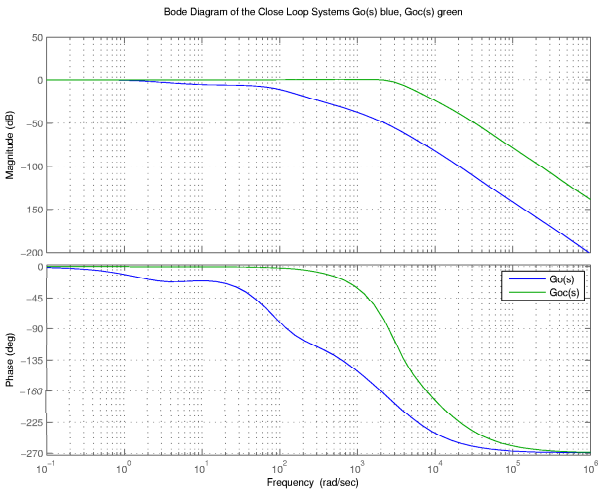

Fig. 12. Bode diagrams of the closed loop system $G_0(s)$, with and without the lead compensator $G_c(s)$.

5.2 Synthesis of the Lead Compensator $G_c(s)$

A lead compensator $G_c(s)$ has been introduced in the pressure control loop for improving the system response and the stability of the controlled system. The compensator has been designed as follows, on the basis of the linear model $G_T(s)$: first of all the static gain K_c has been increased up to the maximum stability gain (see the green line of Fig. 11), then the parameters τ_1 and τ_2 has been calculated according to the following inversion formulas:

$$\tau_1 = \frac{M - \cos\phi}{\overline{\omega}\sin\phi}, \qquad \tau_2 = \frac{\cos\phi - \frac{1}{M}}{\overline{\omega}\sin\phi}$$

where M and ϕ are respectively the magnitude and the lead phase introduced by the compensator $G_c(j\omega)$ at frequency $\overline{\omega}$. These inversion formulas are a mathematical and graphical technique for the optimal design of the lead-lag compensator parameters τ_1 and τ_2. For more details please refer to Marro (1998) and Zanasi (1999). The benefits introduced by the compensator $G_c(s)$ are clearly shown in the Bode diagrams of Fig. 12 (see green line): using the parameters $\tau_1 = 0.001$ s and $\tau_2 = 0.000071$ s,

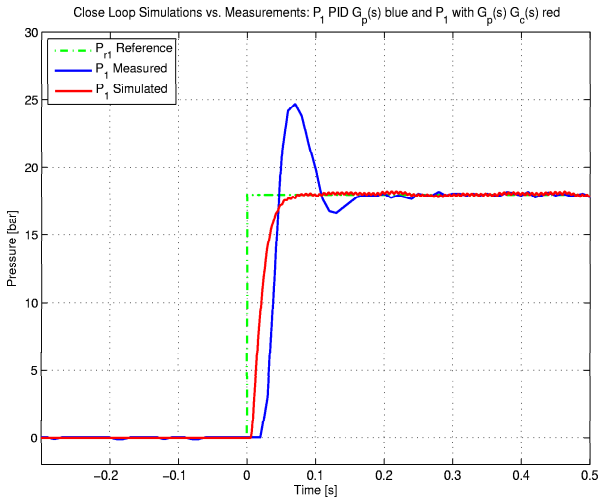

Fig. 13. Comparison between the step response of the simulated POG model with the lead compensator $G_c(s)$ and the real measurements obtained with only the PID controller $G_p(s)$.

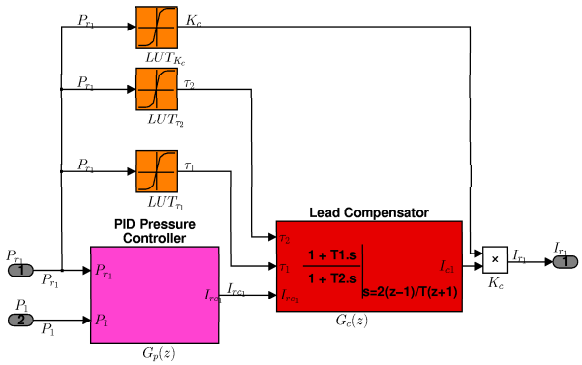

Fig. 14. Dependence of the compensator parameter K_c, τ_1 and τ_2 from the reference pressure P_{r_1}.

the bandwidth of the system has been increased at 3160 rad/s.

6. SIMULATIONS RESULTS COMPARISON

To prove the good performances and the stability of the closed loop system when the compensator $G_c(s)$ is used, a few specific simulations have been performed using the nonlinear POG model. In Fig. 13 it is shown a comparison between the step response of the closed loop system, with the lead compensator $G_c(s)$, and the measurements done on the real system, with only the PID controller $G_p(s)$. From the figure is possible to see that the the parameter K_p of the PID controller has been increased to obtain a better time response, but this introduced a not acceptable overshoot ($S > 35\%$) (blue line). From the figure it is also evident that the step response of the system controlled with the $G_c(s)$ compensator has an improved optimal shape.

To cope with the fact that the controller parameters K_c, τ_1 and τ_2 are dependent on the working point, three Look-up Tables have been introduced in the implementation of the lead compensator $G_c(s)$, see Fig. 14. The three parameters K_c, τ_1 and τ_2 have been expressed as a function of the

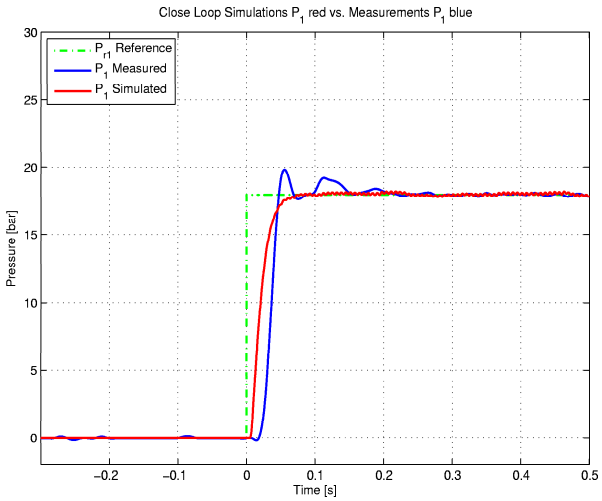

Fig. 15. Comparison between the step response in the closed loop system with the lead compensator: simulated POG model vs. real measurements.

reference pressure P_{r_1} coming from the torque controller:

$$K_c = K_c(P_{r_1}), \quad \tau_1 = \tau_1(P_{r_1}), \quad \tau_2 = \tau_2(P_{r_1})$$

For the software implementation of controller $G_c(s)$ in the digital control unit (ECU), a discrete bilinear transformation $s = \frac{2}{T}\frac{(1-z^{-1})}{(1+z^{-1})}$, with a sampling time of $T = 2$ms has been used.

6.1 Measurements Results Comparison

Due to the nonlinearities of the hydraulic actuator and the process of digitalization of the pressure controller some adaptations of the compensator parameters were necessary. In particular in Fig. 15 it is shown a comparison between the step response of the closed loop system with the lead compensator $G_c(s)$ and the measurements obtained on the real system with the discrete version $G_c(z)$ of compensator $G_c(s)$. The used parameters are: $K_c = 8.5$, $\tau_1 = 0.0122$ s and $\tau_2 = 0.00087$ s. Fig. 15 shows a very good time response for the actuator pressure P_1, $T_s \cong 33$ ms, without having an excessive overshoot ($S < 10\%$).

7. CONCLUSIONS

The control system presented in this paper has been realized by MAGNA STEYR in a prototype demo vehicle named Hybrid Sport Utility Vehicle (HySUV) with four wheels drive, see Fig. 16. The implementation of the presented Hybrid powertrain topology brought MAGNA STEYR to develop a full modular integrated unit, called E4WD module, that covers a wide range of driving possibilities: parallel, serial-hybrid, etc. This solution is suitable for various platforms of vehicle and classes. The E4WD module consists of two electrical motors and four hydraulically actuated multi-disk clutches. An optimized control software, for the regulation of the clutch transfer torque in a hybrid vehicle, has been presented. The controller has been implemented at first with a simple PID and then improved with a properly designed lead compensator. The same software with different parameterizations has been used, in a modular way, to control all the four E4WD module clutches. The modular software has been

Fig. 16. Demo vehicle HySUF based on the platform Daimler ML 350.

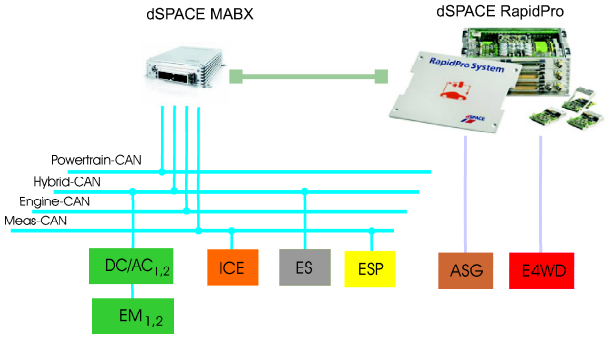

Fig. 17. Schematization of the dSPACE prototyping system in the HySuv demo vehicle.

developed in Matlab/ Simulink, tested in simulation with the POG modelling technique, and then implemented in a dSPACE Micro Auto Box (MABX) connected to the RapidPro hardware, for a proper and direct control of the actuators (see Fig. 17). The MABX system has also been used to communicate, on the CAN buses, with the others vehicle ECUs and to manage the global diagnosis, while the RapidPro stack has been used just as power interface with the actuators and sensors.

7.1 Acknowledgements

Hearty greetings at all the people that directly or indirectly supported the construction of the prototype HySuv Mercedes M-Class, with a special kind of attention at the department ISM of MAGNA STEYR, that developed and supplied internally the whole battery system. Particular thanks also at the company Siemens VDO for the electrical motors and at the company AVL for the engine control. Without all these partners the realization of the demo vehicle would have not been possible.

REFERENCES

A. Schmidhofer, F. Zoehrer, J. Starzinger, K. Erjawetz, V. Hartmann, M. Speiser, *Powertrain Hybridization of a Full Size SUV - A Multifunction Electric 4WD Traction Module.* 19th International AVL Conference "Engine & Environment", Graz, Austria, September 2007.

G. Babiel, *Elektrische Antriebe in der Fahrzeugtechnik.* Vieweg Edition, 2007.

T. Schöberl, F. Gunnar Grein, *Hybrid- Antrieb erfahrbar gemacht.* dSpaceNews, pages 4–8 January 1999.

R. Zanasi, *Power Oriented Modelling of Dynamical System for Simulation.* IMACS Symp. on Modelling and Control of Technological System, Lille, France, May 1991.

R. Zanasi, *Dynamics of a n-links Manipulator by Using Power-Oriented Graph.* SYROCO, Capri, Italy, 1994.

R. Zanasi, G. Sandoni, R. Morselli, A. Visconti, F. Baldet and F. Farachi, *Dynamics models and control of an AMT actuator system.* MECH2K3, Graz, Austria, July, 2003.

R. Cavalcanti, *Modellierung und Regleroptimierung des Kupplungsaktuierungssystems eines Hybridfahrzeugs.* Master Degree Thesis 2007, Fachhochschule Wiener Neustadt für Wirtschaft und Technik in collaboration with the Company MAGNA STEYR Fahrzeugtechnik, May 2007.

G. Sandoni, *Modelling and Control of a Car Driveline.* PhD Thesis A.A. 1999-2002, University of Modena and Reggio Emilia in collaboration with the Company Ferrari SpA, February 2002.

G. Marro and R. Zanasi, *New Formulae and Graphics for Compensator Design.* 1998 IEEE Int. Conference On Control Applications, Triestc, Italy, 1998.

R. Zanasi, *Esercizi Controlli Automatici. Compiti d'esame svolti.* Esculapio Edition, 1999.